Imitating Deep Learning Dynamics

via Locally Elastic Stochastic Differential Equations

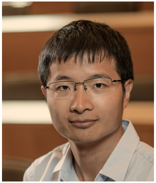

Jiayao Zhang[1,2]   Hua Wang[1]   Weijie J. Su[1]

[1] Department of Statistics   [2] Cognitive Computation Group

NeurIPS 2021

Penn
University *of* Pennsylvania

Contents

Motivation

- A *phenomenological approach* for deep learning.
- We want
  - Big pictures instead of overly-complicated details;
  - Intuitive methods, though may not be fully rigorous without further work;
  - Guidance for future research toward demystifying deep models.

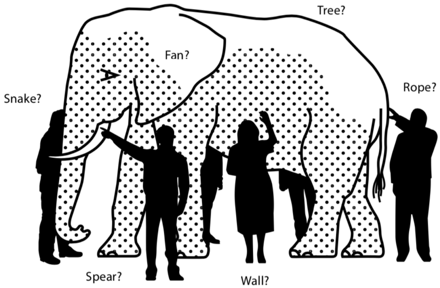

Overview

- Inspired by the *local elasticity* (LE, [HS20, DHS21, CHS20]) phenomenon: training on a sample *x* has a greater effect on samples that are similar to it than on those dissimilar to it.

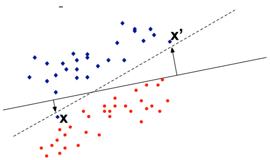

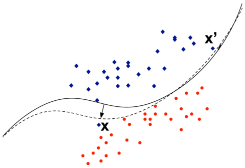

Overview

- Inspired by the *local elasticity* (LE, [HS20, DHS21, CHS20]) phenomenon: training on a sample *x* has a greater effect on samples that are similar to it than on those dissimilar to it.

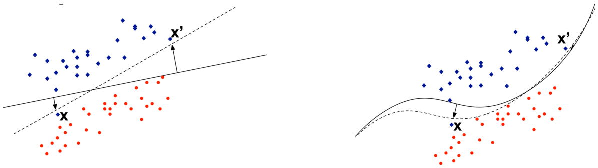

- How to encode this in our model?

Overview

- Inspired by the *local elasticity* (LE, [HS20, DHS21, CHS20]) phenomenon: training on a sample x has a greater effect on samples that are similar to it than on those dissimilar to it.

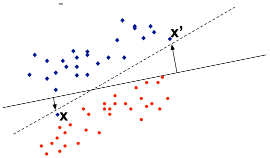

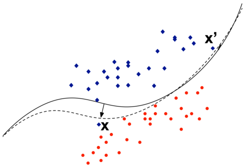

- How to encode this in our model?
- If at the m-th iteration, the l-th sample from the first class is trained, we model

$$\begin{cases} X_i^1(m) = X_i^1(m-1) + h \cdot \alpha X_l^1(m-1) + \text{noise}, \\ X_j^2(m) = X_j^2(m-1) + h \cdot \beta X_l^1(m-1) + \text{noise}. \end{cases} \tag{1}$$

UNIVERSITY *of* PENNSYLVANIA

Overview

- Inspired by the *local elasticity* (LE, [HS20, DHS21, CHS20]) phenomenon: training on a sample x has a greater effect on samples that are similar to it than on those dissimilar to it.

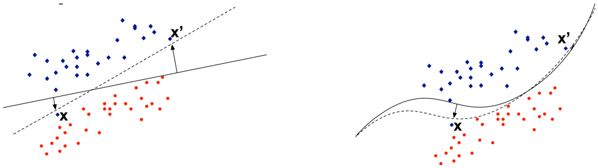

- How to encode this in our model?

- If at the m-th iteration, the l-th sample from the first class is trained, we model

$$\begin{cases} X_i^1(m) = X_i^1(m-1) + h \cdot \alpha X_l^1(m-1) + \text{noise}, \\ X_j^2(m) = X_j^2(m-1) + h \cdot \beta X_l^1(m-1) + \text{noise}. \end{cases} \tag{1}$$

- Then the emergence of LE can be understood as $\gamma := \alpha - \beta$ being large.

Penn
University *of* Pennsylvania

Model Overview (1/2)

- **The LE-SDE: modeling feature dynamics with LE.**

$$\mathrm{d}\tilde{\boldsymbol{X}}(t) = \boldsymbol{M}(t)\tilde{\boldsymbol{X}}(t)\,\mathrm{d}t + \boldsymbol{\Sigma}(t)\,\mathrm{d}\boldsymbol{B}_t, \tag{2}$$

where $\tilde{\boldsymbol{X}}(t) = (\tilde{X}^k(t))_{k=1}^K \in \mathbb{R}^{Kp}$ is the concatenation of p-dimensional feature vectors from K classes. We model the drift

$$\boldsymbol{M}(t) = (\boldsymbol{E}(t) \otimes \boldsymbol{P}) \circ \boldsymbol{H} \tag{3}$$

where the LE matrix $\boldsymbol{E}(t) \in \mathbb{R}^{K\times K}$ models the strength of LE, the sampling matrix $\boldsymbol{P} \in \mathbb{R}^{K\times K}$ models sampling effects, and a "similarity matrix" $\boldsymbol{H} \in \mathbb{R}^{Kp\times Kp}$ (as a K-by-K block matrix) that models the direction features interacts under LE.

The simplest LE matrix can be set to be one with $\alpha(t)$ (intra-class effects) on its diagonal and $\beta(t)$ (inter-class effects) elsewhere.

Penn
University *of* Pennsylvania

Model Overview (2/2)

- **The LE-ODE: dynamics on mean features $\bar{\boldsymbol{X}} = \mathbb{E}_{\text{data}}\tilde{\boldsymbol{X}}$:**

$$\mathrm{d}\bar{\boldsymbol{X}}(t) = \boldsymbol{M}(t)\bar{\boldsymbol{X}}(t)\,\mathrm{d}t = \left(\left(\boldsymbol{E}(t) \otimes \boldsymbol{P}\right) \circ \boldsymbol{H}\right)\bar{\boldsymbol{X}}(t)\,\mathrm{d}t. \tag{4}$$

E.g., given $\boldsymbol{P} = \mathbf{1}_{K\times K}/K$ and the two-parameter LE $\boldsymbol{E}(t)$,

$$\mathrm{d}\underbrace{\begin{bmatrix} \begin{bmatrix} \bar{X}_1^1 \\ \vdots \\ \bar{X}_p^1 \end{bmatrix} \\ \vdots \\ \begin{bmatrix} \bar{X}_1^K \\ \vdots \\ \bar{X}_p^K \end{bmatrix} \end{bmatrix}}_{\bar{\boldsymbol{X}}(t)} = \frac{1}{K}\underbrace{\begin{bmatrix} \alpha(t) & \beta(t) & \dots & \beta(t) \\ \beta(t) & \alpha(t) & \dots & \beta(t) \\ \vdots & \vdots & \dots & \vdots \\ \beta(t) & \dots & \dots & \alpha(t) \end{bmatrix}}_{\boldsymbol{E}(t)} \circ \underbrace{\begin{bmatrix} \boldsymbol{H}_{11} & \boldsymbol{H}_{12} & \dots & \boldsymbol{H}_{1K} \\ \boldsymbol{H}_{21} & \boldsymbol{H}_{22} & \dots & \boldsymbol{H}_{2K} \\ \vdots & \dots & \dots & \vdots \\ \boldsymbol{H}_{K1} & \boldsymbol{H}_{K2} & \dots & \boldsymbol{H}_{KK} \end{bmatrix}}_{\boldsymbol{H}} \begin{bmatrix} \begin{bmatrix} \bar{X}_1^1 \\ \vdots \\ \bar{X}_p^1 \end{bmatrix} \\ \vdots \\ \begin{bmatrix} \bar{X}_1^K \\ \vdots \\ \bar{X}_p^K \end{bmatrix} \end{bmatrix} \mathrm{d}t. \tag{5}$$

Main Results

- **Separation Theorem:** features are asymptotically linearly separable if there is LE ("$\alpha(t) > \beta(t)$") for PSD $\boldsymbol{H}$ with positive diagonals.

- **Modeling choices for $\boldsymbol{H} = (\boldsymbol{H}_{ij})_{ij}$ matrix.**

Model	$\boldsymbol{H}_{ij}$	Remark
I-model	$\boldsymbol{I}_p$	Isotropic Feature Model
L-model	$\bar{\boldsymbol{H}}^j = \boldsymbol{d}_j \boldsymbol{d}_j^\top / \Vert \boldsymbol{d}_j \Vert_2^2$	Logits-as-Features Model

Table 1: Modeling choices for $\boldsymbol{H}$, where $\boldsymbol{d}_j = \boldsymbol{e}_j - \frac{1}{K}\mathbf{1}_p$ for $j \in [K]$.

- **Simulating genuine dynamics with the LE matrix estimated.**

Contents

The Separation Theorem

Theorem (Separation of LE-SDE)

Suppose $\gamma(t) = \alpha(t) - \beta(t) > 0$, assume $\boldsymbol{H} = (\boldsymbol{H}_{ij})_{ij}$ is positive semi-definite (PSD) with positive diagonal entries. As $t \to \infty$, we have

1. *if $\gamma(t) = \omega(1/t)$, the features are separable with probability tending to 1;*
2. *if $\gamma(t) = o(1/t)$, and the number of per-class-feature n tending to ∞ at an arbitrarily slow rate, the features are asymptotically pairwise separable with probability 0.*

Here, $\gamma(t) = \omega(1/t)$ stands for $\gamma(t) \gg 1/t$ as $t \to \infty$. For example, $1/t^{0.5} = \omega(1/t)$ and $(t \ln t)^{-1} = o(1/t)$ as $t \to \infty$.

Proof Sketch

- Substituting back the solution of the LE-ODE

$$\bar{\boldsymbol{X}}_t = \bar{\boldsymbol{X}}_0 + \sum_{i=1}^{Kp} c_i \boldsymbol{u}_i \, \mathrm{e}^{\mu_i t}, \quad \bar{\boldsymbol{X}}_0 = \sum_{i=1}^{Kp} c_i \boldsymbol{u}_i, \tag{6}$$

 to the LE-SDE, we have

$$\begin{aligned} \tilde{\boldsymbol{X}}^k(t) &= \tilde{\boldsymbol{X}}^k(0) + \boldsymbol{M}_t \bar{\boldsymbol{X}}(t) - \mathbb{E}[\tilde{\boldsymbol{X}}^k(0)] + \boldsymbol{\Sigma}_k^{\frac{1}{2}}(t) \boldsymbol{W}^k(t) \\ &= \tilde{\boldsymbol{X}}^k(0) + \sum_{i=1}^{Kp} c_i \mu_i \boldsymbol{u}_i^k \, \mathrm{e}^{\mu_i t} - \sum_{i=1}^{Kp} c_i \boldsymbol{u}_i^k + \boldsymbol{\Sigma}_k^{\frac{1}{2}} \boldsymbol{W}^k(t), \end{aligned} \tag{7}$$

- To prove separation, it suffices to identify a direction $\boldsymbol{\nu}$ such that

$$\left\langle \tilde{\boldsymbol{X}}^k(t) - \tilde{\boldsymbol{X}}^l(t), \boldsymbol{\nu} \right\rangle > 0, \quad \text{w.p.} \rightarrow 1 \text{ as } t \rightarrow \infty, \quad \forall k \neq l. \tag{8}$$

- Using Gaussian tail bound to obtain the rates; using nullity theorems to show $\boldsymbol{\nu}$ can be chosen independent of the class indices.

Penn
University *of* Pennsylvania

Corollary

Neural collapse [PHD20, FHLS21] is a recent phenomenological finding on the geometry of logits of DNNs at convergence: they tend to form equiangular tight frames (ETFs).

Proposition (Neural Collapse of the LE-ODE)

Under L-model and the same setup as in Theorem 1, if $\gamma(t) > 0$ and there exists some $T > 0$ such that $B(t) < 0$ for $t \geq T$, then $\left\{\bar{\boldsymbol{X}}^k(t)/\|\bar{\boldsymbol{X}}^k(t)\|\right\}_{k=1}^{K}$ forms an ETF as $t \to \infty$.

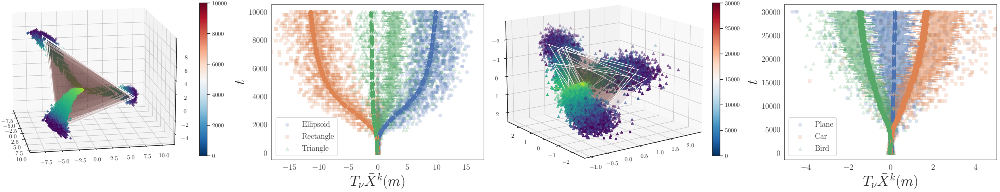

(a) GeoMNIST in $\mathbb{R}^3$. (b) GeoMNIST in $\mathbb{R}$. (c) CIFAR in $\mathbb{R}^3$. (d) CIFAR in $\mathbb{R}$.

Justifications for Linearization (1/5)

- **The genuine dynamics of logits.**

$$\boldsymbol{X}_i^k(m) - \boldsymbol{X}_i^k(m-1) \approx h \left[\frac{\partial \boldsymbol{X}_i^k(m-1)}{\partial \boldsymbol{w}} \frac{\partial \boldsymbol{X}_{J_m}^{L_m}}{\partial \boldsymbol{w}}^\top \left(\boldsymbol{e}_{L_m} - \mathrm{softmax}(\boldsymbol{X}_{J_m}^{L_m}) \right) \right]. \tag{9}$$

- **First approximation: decoupling in an expectation.**

$$\begin{aligned} \mathrm{d}\tilde{\boldsymbol{X}}_t^k &\approx \mathbb{E}_{L \sim \mathrm{U}([K])} \left[\mathbb{E}_{\tilde{\boldsymbol{X}} \sim \mathcal{D}_t^L} \left[\frac{\partial \boldsymbol{X}_i^k(m-1)}{\partial \boldsymbol{w}} \frac{\partial \tilde{\boldsymbol{X}}}{\partial \boldsymbol{w}}^\top \left(\boldsymbol{e}_L - \mathrm{softmax}(\tilde{\boldsymbol{X}}) \right) \right] \right] \mathrm{d}t + \boldsymbol{\Sigma}_t^{\frac{1}{2}} \, \mathrm{d}\boldsymbol{W}_t, \\ &\approx \frac{1}{K} \sum_L \left(\left[\mathbb{E}_{\tilde{\boldsymbol{X}}' \sim \mathcal{D}_t^k, \tilde{\boldsymbol{X}} \sim \mathcal{D}_t^L} \frac{\partial \tilde{\boldsymbol{X}}'}{\partial \boldsymbol{w}} \frac{\partial \tilde{\boldsymbol{X}}}{\partial \boldsymbol{w}}^\top \right] \left(\boldsymbol{e}_L - \mathrm{softmax}(\bar{\boldsymbol{X}}_t^L) \right) \right) \mathrm{d}t + \boldsymbol{\Sigma}_t^{\frac{1}{2}} \, \mathrm{d}\boldsymbol{W}_t, \\ &= \frac{1}{K} \sum_L \left(\Theta_{k,L} \left(\boldsymbol{e}_L - \mathrm{softmax}(\bar{\boldsymbol{X}}_t^L) \right) \right) \mathrm{d}t + \boldsymbol{\Sigma}_t^{\frac{1}{2}} \, \mathrm{d}\boldsymbol{W}_t. \end{aligned} \tag{10}$$

Justifications for Linearization (2/5)

- **Linearize the drift F around the mean at each time.**

$$F(\tilde{\boldsymbol{X}}(t), t) := \Theta(t)\left(\left[e_k - \sigma(\tilde{\boldsymbol{X}}^k(t))\right]_{k=1}^{K}\right), \tag{11}$$

$$F(\tilde{\boldsymbol{X}}(t), t) \approx \tilde{F}(\tilde{\boldsymbol{X}}(t), t) := F(\varphi(t), t) + \nabla_X F(\varphi(t), t)\left(\tilde{\boldsymbol{X}}(t) - \varphi(t)\right), \tag{12}$$

where $\varphi(t) := \bar{\boldsymbol{X}}(t)$, $J = \nabla_X F = J$ is a block diagonal matrix $J = (J_{kk})$ with $J_{kk} = J_k := \mathrm{diag}(\bar{p}_k) - \bar{p}_k\bar{p}_k^T$, here we write

$$p = (p_k)_{k=1}^K \in \mathbb{R}^{Kp}, \quad p_k := \sigma(\tilde{\boldsymbol{X}}^k(t)) \in \mathbb{R}^p, \quad k \in [K], \tag{13}$$

and similarly

$$\bar{p} = (\bar{p}_k)_{k=1}^K \in \mathbb{R}^{Kp}, \quad \bar{p}_k := \sigma(\bar{\boldsymbol{X}}^k(t)) \in \mathbb{R}^p, \quad k \in [K]. \tag{14}$$

Penn
University *of* Pennsylvania

Justifications for Linearization (3/5)

- **Linearize the drift F around the mean at each time (cont'd).**

$$\begin{aligned}\tilde{F}(\tilde{\boldsymbol{X}}(t), t) &= \Theta(t)\left([e_k - \bar{p}_k]_k + J(t)(\tilde{\boldsymbol{X}}(t) - \varphi(t))\right) \\ &= \Theta(t)\left(J(t)X(t) + [e_k - \bar{p}_k + J_k\varphi_k(t)]_k\right).\end{aligned} \tag{15}$$

Define $\Psi : \mathbb{R}^{Kp} \to \mathbb{R}^{Kp} : z \mapsto [e_k - \sigma(z_k)]_k$ and write $\Psi_k : \mathbb{R}^p \to \mathbb{R}^p$ to be the k-th component of Ψ, expand $\Psi(z)$ around $\varphi(t)$ for each t:

$$\Psi = \Psi(\varphi) + J(t)\varphi - J(\varphi)z + o\left(\|z - \varphi\|\right), \tag{16}$$

or

$$\Psi(\varphi) + J(t)\varphi = \Psi(z) + J(\varphi)z + o\left(\|z - \varphi\|\right). \tag{17}$$

This implies that

$$\tilde{F} = \Theta(t)J(t)\tilde{\boldsymbol{X}}(t) + \Theta(t)R(t), \quad R(t; z) := \Psi(z) + J(t)z + o\left(\|z - \varphi(t)\|\right). \tag{18}$$

Penn
University of Pennsylvania

Justifications for Linearization (4/5)

- **Point z for expansion.**
  - **Around initialization: constant residue.** Let $z = u := c \cdot [\mathbf{1}_K/K]_{k=1}^K$ be a scaling of vectors of ones where c is some fixed constant. Then each of the K components of $\sigma(u)$ assigns approximately the same probability ($1/K$) for every label. Furthermore, $u \in \operatorname{Ker} J(t)$ for all t hence the residue $R(t; u) = \Psi(u) + o\left(\|z - \varphi(t)\|\right)$ is a constant vector.
  - **Around convergence: vanishing residue.** Given that the model converges, $\varphi_\infty := \varphi(\infty)$ is finite. Let $z = \varphi_\infty$, under the effective training assumption, $\|\Psi(\varphi_\infty)\| \approx 0$ by construction. Hence the residue $R(t; \varphi_\infty) = J(t)\varphi_\infty + o\left(\|\varphi(t) - \varphi_\infty)\|\right)$. Here the $o(\cdot)$ term converges to 0 as training progresses, leaving us a term that is asymptotically equivalent to $v = (v_k)_{k=1}^K := J(\varphi_\infty)\varphi_\infty \in \mathbb{R}^{K^2}$, where $v_k = [(z_{k,i} - \sum_{j=1}^K p_{k,j} z_{k,j})p_i]_{i=1}^K \in \mathbb{R}^K \approx \mathbf{0}_K$ under the effective training assumption. In this regime, the residue $o\left(\|\varphi(t) - \varphi_\infty\|\right)$ eventually vanishes.

University of Pennsylvania

Justifications for Linearization (5/5)

Summary of Approximations

- Decoupling inside an expectation.
- Linearize the drift around the mean $\bar{\boldsymbol{X}}$.
- First-order expansion around convergence.

Contents

Setup

- **Datasets and Models.**

Setup

- **Datasets and Models.**
  - GeoMNIST: $K = 3$ classes of simple geometric shapes (Rectangle, Ellipsoid, and Triangle).

Setup

- **Datasets and Models.**
  - GeoMNIST: $K = 3$ classes of simple geometric shapes (Rectangle, Ellipsoid, and Triangle).
  - CIFAR-10: 5000 training samples and 1000 validation samples per class, with the total number of classes $K \in [2, 3]$.

Setup

- **Datasets and Models.**
  - GeoMNIST: $K = 3$ classes of simple geometric shapes (Rectangle, Ellipsoid, and Triangle).
  - CIFAR-10: 5000 training samples and 1000 validation samples per class, with the total number of classes $K \in [2, 3]$.
- **Training Configurations.**

Setup

- **Datasets and Models.**
  - GeoMNIST: $K = 3$ classes of simple geometric shapes (Rectangle, Ellipsoid, and Triangle).
  - CIFAR-10: 5000 training samples and 1000 validation samples per class, with the total number of classes $K \in [2, 3]$.
- **Training Configurations.**
  - Variants of the AlexNet model ([KSH12]): two convolutional layers and three fully-connected layers activated by $\texttt{ReLU}$.

Setup

- **Datasets and Models.**
  - GeoMNIST: $K = 3$ classes of simple geometric shapes (Rectangle, Ellipsoid, and Triangle).
  - CIFAR-10: 5000 training samples and 1000 validation samples per class, with the total number of classes $K \in [2, 3]$.
- **Training Configurations.**
  - Variants of the AlexNet model ([KSH12]): two convolutional layers and three fully-connected layers activated by $\mathtt{ReLU}$.
  - All models are trained for $T = 10^5$ iterations (for GeoMNIST) or $T = 3 \times 10^5$ iterations (for CIFAR) with a learning rate of 0.005 and a batch size of 1 under the softmax cross-entropy loss. Models on GeoMNIST converged with training and validation losses to zero, and those on CIFAR to validation accuracies greater than 90%.

LE Coefficients Estimation

- **Estimation Procedure.** Define $A(t) = \int_0^t \alpha(\tau)\,\mathrm{d}\tau$, $B(t) = \int_0^t \beta(\tau)\,\mathrm{d}\tau$, write out exact solutions under the I-model and the L-model, we can estimate

$$
\begin{aligned}
&(\text{I-model}) \quad \begin{cases} \hat{A}(t) &= \operatorname{avg} \operatorname{avg}_k \log \left| \frac{\check{\boldsymbol{x}}(\bar{\boldsymbol{x}}^k - \check{\boldsymbol{x}})^{K-1}}{\boldsymbol{c}_0 \boldsymbol{c}_k^{K-1}} \right|, \\ \hat{B}(t) &= -\operatorname{avg} \operatorname{avg}_k \log \left| \frac{\boldsymbol{c}_0}{\boldsymbol{c}_k} \frac{\bar{\boldsymbol{x}}^k - \check{\boldsymbol{x}}}{\check{\boldsymbol{x}}} \right|, \end{cases} \quad \check{\boldsymbol{X}}_t := \operatorname{avg}_l \bar{\boldsymbol{X}}_t^l, \\
&(\text{L-model}) \quad \begin{cases} \hat{A}(t) &= A'(t) + 2B'(t), \\ \hat{B}(t) &= 2(B'(t) - A'(t)), \end{cases} \quad \begin{cases} A'(t) &:= \log \left| \left\langle \bar{\boldsymbol{X}}^\top \boldsymbol{v}_1 - 1 \right\rangle \right|, \\ B'(t) &:= \log \left| \left\langle \bar{\boldsymbol{X}}^\top \left(\boldsymbol{v}_2 - \frac{4}{3} \boldsymbol{v}_1 \right) \right\rangle \right|, \end{cases}
\end{aligned} \tag{19}
$$

where $\operatorname{avg}_l(\cdot)$ denotes averaging over axis l, and $\operatorname{avg}(\cdot)$ averaging all elements.

LE Coefficients Estimation

- **Estimation Procedure.** Define $A(t) = \int_0^t \alpha(\tau)\,\mathrm{d}\tau$, $B(t) = \int_0^t \beta(\tau)\,\mathrm{d}\tau$, write out exact solutions under the I-model and the L-model, we can estimate

$$\begin{aligned}
&\text{(I-model)} \quad \begin{cases} \hat{A}(t) &= \operatorname{avg} \operatorname{avg}_k \log \left| \frac{\check{\boldsymbol{x}}(\bar{\boldsymbol{x}}^k - \check{\boldsymbol{x}})^{K-1}}{\boldsymbol{c}_0 \boldsymbol{c}_k^{K-1}} \right|, \\ \hat{B}(t) &= -\operatorname{avg} \operatorname{avg}_k \log \left| \frac{\boldsymbol{c}_0}{\boldsymbol{c}_k} \frac{\bar{\boldsymbol{x}}^k - \check{\boldsymbol{x}}}{\check{\boldsymbol{x}}} \right|, \end{cases} \quad \check{\boldsymbol{X}}_t := \operatorname{avg}_l \bar{\boldsymbol{X}}_t^l, \\
&\text{(L-model)} \quad \begin{cases} \hat{A}(t) &= A'(t) + 2B'(t), \\ \hat{B}(t) &= 2(B'(t) - A'(t)), \end{cases} \quad \begin{cases} A'(t) &:= \log \left| \left\langle \bar{\boldsymbol{X}}^\top \boldsymbol{v}_1 - 1 \right\rangle \right|, \\ B'(t) &:= \log \left| \left\langle \bar{\boldsymbol{X}}^\top \left(\boldsymbol{v}_2 - \frac{4}{3}\boldsymbol{v}_1\right) \right\rangle \right|, \end{cases}
\end{aligned} \tag{19}$$

  where $\operatorname{avg}_l(\cdot)$ denotes averaging over axis l, and $\operatorname{avg}(\cdot)$ averaging all elements.

- Main idea: eigenvectors of the Kp-by-Kp drift matrix $M(t)$ as concatenations of K vectors in $\mathbb{R}^p$ and construct their linear combinations such that one or more independent components in the solution vanishes.

University of Pennsylvania

LE Coefficients Estimation

- **Estimation Procedure.** Define $A(t) = \int_0^t \alpha(\tau)\,\mathrm{d}\tau$, $B(t) = \int_0^t \beta(\tau)\,\mathrm{d}\tau$, write out exact solutions under the I-model and the L-model, we can estimate

$$
\begin{aligned}
&(\text{I-model}) \quad \begin{cases} \hat{A}(t) &= \operatorname{avg}\operatorname{avg}_k \log \left| \dfrac{\check{\boldsymbol{x}}(\bar{\boldsymbol{x}}^k - \check{\boldsymbol{x}})^{K-1}}{c_0 c_k^{K-1}} \right|, \\ \hat{B}(t) &= -\operatorname{avg}\operatorname{avg}_k \log \left| \frac{c_0}{c_k} \frac{\bar{\boldsymbol{x}}^k - \check{\boldsymbol{x}}}{\check{\boldsymbol{x}}} \right|, \end{cases} \quad \check{\boldsymbol{X}}_t := \operatorname{avg}_l \bar{\boldsymbol{X}}_t^l, \\
&(\text{L-model}) \quad \begin{cases} \hat{A}(t) &= A'(t) + 2B'(t), \\ \hat{B}(t) &= 2(B'(t) - A'(t)), \end{cases} \quad \begin{cases} A'(t) &:= \log \left| \left\langle \bar{\boldsymbol{X}}^\top \boldsymbol{v}_1 - 1 \right\rangle \right|, \\ B'(t) &:= \log \left| \left\langle \bar{\boldsymbol{X}}^\top \left(\boldsymbol{v}_2 - \frac{4}{3}\boldsymbol{v}_1 \right) \right\rangle \right|, \end{cases}
\end{aligned} \tag{19}
$$

  where $\operatorname{avg}_l(\cdot)$ denotes averaging over axis l, and $\operatorname{avg}(\cdot)$ averaging all elements.

- Main idea: eigenvectors of the Kp-by-Kp drift matrix $M(t)$ as concatenations of K vectors in $\mathbb{R}^p$ and construct their linear combinations such that one or more independent components in the solution vanishes.

- Obtain $\hat{\alpha}(t)$ and $\hat{\beta}(t)$ using the Savitzky-Golay filter.

LE Coefficients Estimation

- **Estimation Procedure.** Define $A(t) = \int_0^t \alpha(\tau)\,\mathrm{d}\tau$, $B(t) = \int_0^t \beta(\tau)\,\mathrm{d}\tau$, write out exact solutions under the I-model and the L-model, we can estimate

$$
\begin{aligned}
&(\text{I-model}) \quad \begin{cases} \hat{A}(t) &= \operatorname{avg}\operatorname{avg}_k \log \left| \frac{\check{\boldsymbol{x}}(\bar{\boldsymbol{x}}^k - \check{\boldsymbol{x}})^{K-1}}{c_0 c_k^{K-1}} \right|, \\ \hat{B}(t) &= -\operatorname{avg}\operatorname{avg}_k \log \left| \frac{c_0}{c_k} \frac{\bar{\boldsymbol{x}}^k - \check{\boldsymbol{x}}}{\check{\boldsymbol{x}}} \right|, \end{cases} \quad \check{\boldsymbol{x}}_t := \operatorname{avg}_l \bar{\boldsymbol{x}}_t^l, \\
&(\text{L-model}) \quad \begin{cases} \hat{A}(t) &= A'(t) + 2B'(t), \\ \hat{B}(t) &= 2(B'(t) - A'(t)), \end{cases} \quad \begin{cases} A'(t) &:= \log \left| \left\langle \bar{\boldsymbol{x}}^\top \boldsymbol{v}_1 - 1 \right\rangle \right|, \\ B'(t) &:= \log \left| \left\langle \bar{\boldsymbol{x}}^\top \left(\boldsymbol{v}_2 - \frac{4}{3}\boldsymbol{v}_1\right) \right\rangle \right|, \end{cases}
\end{aligned} \tag{19}
$$

where $\operatorname{avg}_l(\cdot)$ denotes averaging over axis l, and $\operatorname{avg}(\cdot)$ averaging all elements.

- Main idea: eigenvectors of the Kp-by-Kp drift matrix $M(t)$ as concatenations of K vectors in $\mathbb{R}^p$ and construct their linear combinations such that one or more independent components in the solution vanishes.
- Obtain $\hat{\alpha}(t)$ and $\hat{\beta}(t)$ using the Savitzky-Golay filter.
- *Tail index* $r_\alpha := \sup_s \{s : \lim_{t\to\infty} \alpha(t) \cdot t^s < \infty\}$, estimated by $\hat{r}_\alpha = 1 - \operatorname{avg}_{T-1000 \le t \le T} \frac{\log \alpha(t)}{\log(1+t)}$.

LE Coefficient Estimation

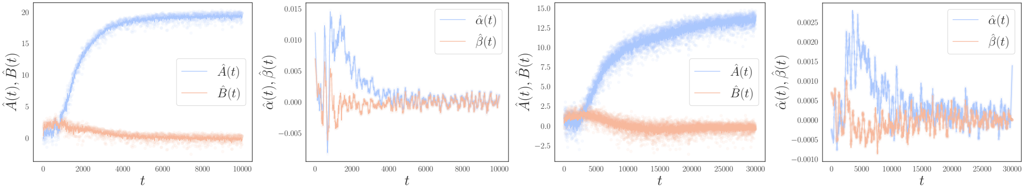

(a) GeoMNIST (I-model). (b) GeoMNIST (I-model). (c) CIFAR (I-model). (d) CIFAR (I-model).

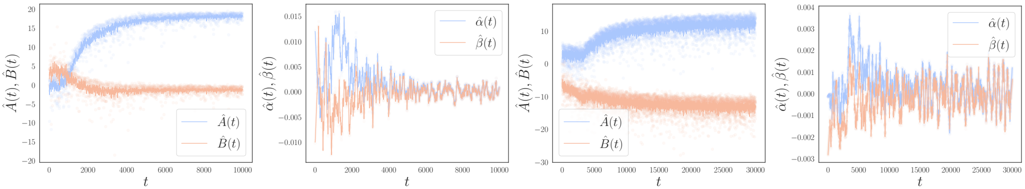

(e) GeoMNIST (L-model). (f) GeoMNIST (L-model). (g) CIFAR (L-model). (h) CIFAR (L-model).

Figure 2: **Estimated $\hat{A}(t)$, $\hat{B}(t)$, $\alpha(t)$, and $\beta(t)$.** The first row was estimated using I-model and the second L-model; the first two columns are on GeoMNIST and the last two on CIFAR. The first and third rows show $\hat{A}(t)$ and $\hat{B}(t)$ and the other two rows $\hat{\alpha}(t)$ and $\hat{\beta}(t)$.

University of Pennsylvania

Verifying the Separation Theorem

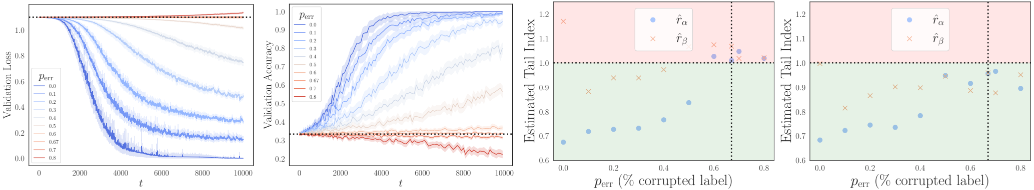

(a) Validation loss. (b) Validation accuracy. (c) I-model. (d) L-model.

Figure 3: **Phase transition of separability over label pollution ratio $p_{\rm err}$. (a)—(b)** Validation loss and accuracy suggest separation fails for $p_{\rm err} \geq p^*_{\rm err} = 2/3$. The dashed line in (a) carries the value at initialization and overlaps with the case where $p_{\rm err} = 0.6$; the dashed line in (b) is $p^*_{\rm err} = 2/3$, when labels are assigned completely at random. **(c)—(d)** Tail indices of $\alpha(t)$ and $\beta(t)$ estimated using the I-model and L-model resp. Although the case for the L-model does not exhibit a clear phase transition, we note around $p_{\rm err} \approx 2/3$, the tail index of $\hat{\beta}(t)$ begins to dominate that of $\hat{\alpha}(t)$.

Penn
University *of* Pennsylvania

Simulating Dynamics via LE-SDE

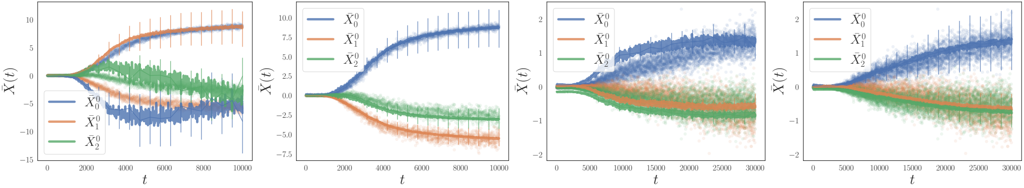

(a) GeoMNIST (l-model). (b) GeoMNIST (L-model). (c) CIFAR (l-model). (d) CIFAR (L-model).

Figure 4: **Simulated LE-ODE solutions versus genuine dynamics.** We use $\hat{\alpha}(t)$ and $\hat{\beta}(t)$ estimated from l-model ((a) and (c)) or L-model, ((b) and (d)) and numerically simulate the solution under the L-model. The results were overlaid with true dynamics from neural nets. We note L-model in general imitated true dynamics reasonably well.

Residues of Simulating Dynamics via LE-SDE

We measure the goodness-of-fit via relative difference (RD, the lower the better) defined for each class $k \in [K]$ as

$$\mathrm{RD_k}(t) := \frac{\left\|\bar{\boldsymbol{X}}^k(t) - \bar{\boldsymbol{Y}}^k(t)\right\|_{\boldsymbol{H}^k}}{\left(\left\|\bar{\boldsymbol{X}}^k(t)\right\|_2 + \left\|\bar{\boldsymbol{Y}}^k(t)\right\|_2\right)/2}, \tag{20}$$

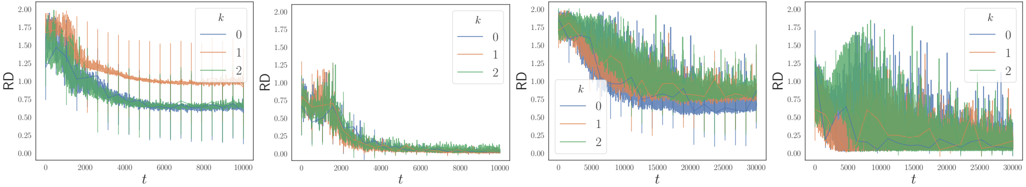

(a) GeoMNIST (I-model). (b) GeoMNIST (L-model). (c) CIFAR (I-model). (d) CIFAR (L-model).

Figure 5: **Relative difference RD_k between genuine and simulated dynamics.** Note that the L-model performs better than I-model throughout training and better captures the later stages of the training (indicated by decreasing RD).

Contents

University of Pennsylvania

Take-Home Messages

- A phenomenological approach: modeling feature dynamics via SDEs that encodes local elasticity. LE-SDE/ODE can model feature dynamics reasonably well; but to close the gap, we may need to go beyond linearity.
- LE is important for separation of features.
- The LE-SDE can be used to imitate the true dynamics once the LE strengths are estimated.

Future Works

- **General LE Matrix.** A similar result as in Theorem 1 may be expected for symmetric but no necessarily semi-definite LE matrices $\boldsymbol{E}(t)$.
- **Mini-batch Training, Imbalanced Datasets, and Label Corruptions.** Generalizing the drift matrix to $\boldsymbol{M}_t = (\boldsymbol{E}_t \otimes \boldsymbol{P}) \circ \boldsymbol{H}/K$ for a K-by-K doubly stochastic matrix $\boldsymbol{P}$ can be used to model various sampling effects.
- **Beyond L-model for Imitating Genuine Dynamics of DNNs.** Although the L-model is shown to be able to mimic the real dynamics reasonably well, we postulate that a more precise model might have its (i, j)-th block encode the other directions other than $\boldsymbol{d}_j$.
- **Finer-Grained Analysis and the Covariance Structure.**
- **Two-Stage Behavior and Exit-Time Analysis.**

Penn
UNIVERSITY *of* PENNSYLVANIA

Acknowledgements

This work was supported in part by NSF through CCF-1934876, an Alfred Sloan Research Fellowship, the Wharton Dean's Research Fund, and ONR Contract N00014-19-1-2620. We would like to thank Dan Roth and the Cognitive Computation Group at the University of Pennsylvania for stimulating discussions and for providing computational resources.

References

Shuxiao Chen, Hangfeng He, and Weijie Su, *Label-aware neural tangent kernel: Toward better generalization and local elasticity*, Advances in Neural Information Processing Systems, vol. 33, 2020, pp. 15847–15858.

Zhun Deng, Hangfeng He, and Weijie Su, *Toward better generalization bounds with locally elastic stability*, Proceedings of the 38th International Conference on Machine Learning, Proceedings of Machine Learning Research, vol. 139, 2021, pp. 2590–2600.

C. Fang, H. He, Q. Long, and W. J. Su, *Exploring deep neural networks via layer-peeled model: Minority collapse in imbalanced training*, Proceedings of the National Academy of Sciences (2021).

Hangfeng He and Weijie Su, *The local elasticity of neural networks*, International Conference on Learning Representations, 2020.

Alex Krizhevsky, Ilya Sutskever, and Geoffrey E Hinton, *Imagenet classification with deep convolutional neural networks*, Advances in Neural Information Processing Systems **25** (2012), 1097–1105.

Vardan Papyan, X. Y. Han, and David L. Donoho, *Prevalence of neural collapse during the terminal phase of deep learning training*, Proceedings of the National Academy of Sciences **117** (2020), no. 40, 24652–24663.